Scheme for topological single electron pumping assisted by Majorana fermions

Qi-Feng Liang,[1,2] Zhi Wang,[1] and Xiao Hu[1]
[1]*International Center for Materials Nanoarchitectonics, National Institute for Materials Science, Tsukuba 305-0044, Japan*
[2]*Department of Physics, Shaoxing University, Shaoxing 312000, China*
(Received 3 November 2012; revised manuscript received 9 May 2014; published 24 June 2014)

Single electron pumping based on the topological property of Majorana fermions (MFs), which specify the parity of electron number, is proposed. The setup consists of a quantum dot (QD) and two NOT gates each with four nanotopological superconductors (TSs) connected by constriction junctions and an additional vortex located in the loop of TSs. Operation is performed by gate voltages at constriction junctions. The condition of QD energy for sequential electron pumping is derived in terms of interactions among TSs, indicating that the QD energy may lie outside the energies of electrodes, which is unique as compared with other existing pumping mechanisms. The essence of the present topological single electron pumping lies in the nonlocal property of MFs, which makes crossing between quasiparticle levels possible and electrically controllable. The operation of the NOT gate is demonstrated, explicitly solving the time-dependent Bogoliubov-de Gennes equation for a microscopic model.

DOI: 10.1103/PhysRevB.89.224514 PACS number(s): 71.10.Pm, 03.67.Lx, 74.45.+c, 74.78.Fk

I. INTRODUCTION

In electronics-based computers, computation is performed based on motions of submillions of electrons, where the accuracy of bit manipulation relies on the statistics of a huge number of electrons. If one can control electrons one by one at given instants, a single electron bit may be achieved, which reduces the energy consumption to the limit. This technology is also important for forming the metrology triangle of Ohm's law: the quantum Hall effect discovered by von Klitzing works as the conductance standard [1], and the Josephson effect provides the voltage standard [2], while realization of a precise current standard remains a challenge [3].

Manipulation of individual electrons in condensed matters is not easy since the wavelength of electrons is comparable with their separation. One way to transport single electrons is to use quantum tunneling. In order to avoid otherwise random processes in time, quantum dots (QDs) are introduced to puncture successfully the time for electrons to tunnel [4–8]. Charge pumpings with precisely controlled current have been realized by tuning the potential of a QD with a given frequency, which works as a "turnstile" for electrons [9,10]. Another important category of charge pumping was formulated [11,12] and developed by many subsequent proposals, based on topology of gapped systems, where the integer numbers of electrons given by topological index are transported when the system moves around a closed loop in the relevant parameter space.

In a topological superconductor (TS) characterized by Majorana fermions (MFs) as zero-energy quasiparticle excitations, the ground state exhibits degeneracy with respect to the parity of electron number [13–29]. Processes for reversing parity in segments and/or circles of a one-dimensional topological superconductor have been proposed [30,31]. The idea of parity pumping was discussed in a topological superconductor-metal junction where the global gap in energy spectrum is suppressed due to the metal lead [32].

In the present work, we compose a protocol for single electron pumping in terms of the topological property of MFs, with the energy gap always open, which features the topological protection. Our setup consists of four TSs, each carrying a vortex and connected by constriction junctions; there is an additional vortex inside the loop of TSs (see Fig. 1). In order to reveal the topological property of the system, we first attach another TS to the device. We show that the edge MF of this TS can be driven in a controlled way around the loop of the four TSs by switching on and off gate voltages at constriction junctions in the designed sequence. After this process, the parity of this TS is flipped since the edge MF acquires a π phase because of the vortex at the center of the device. Therefore, one can consider this TS as a MF qubit and the device of four TSs as a NOT gate. Numerical simulations based on the time-dependent Bogloliubov-de Gennes (TDBdG) equation [33] are performed, which confirm successfully the quantum protection and phase coherence during the whole process. We then demonstrate that two NOT gates work for single electron pumping when a QD with a Coulomb blockade effect is attached between them with the on-site energy of the QD adjusted appropriately.

The remaining part of this paper is organized as follows. We discuss in Sec. II the dynamics of an edge MF in a MF qubit driven through the NOT gate. Then we reveal the relation satisfied by the interactions in the NOT gate in Sec. III. Based on the property of the NOT gate, we formulate in Sec. IV the topological single electron pumping by attaching a QD to two NOT gates and give explicitly the energy regime for the QD. In Sec. V, it is clarified that the function of the NOT gate can be understood as a quantum interference between two MFs. Discussions are presented in Sec. VI, with a summary given in Sec. VII.

II. NOT GATE FOR MF QUBIT

A topological superconducting state can be achieved in a heterostructure of a s-wave superconductor (SC), spin-orbit coupling semiconductor, and ferromagnetic insulator with one vortex at the sample center, where one MF appears at the vortex core and another MF appears at the sample edge [25,33]. In the present device, four finite TSs are positioned on a common SC substrate. The core MFs are stable and do not participate in the phenomena discussed below (strictly speaking there are exponentially small contributions, which can be neglected

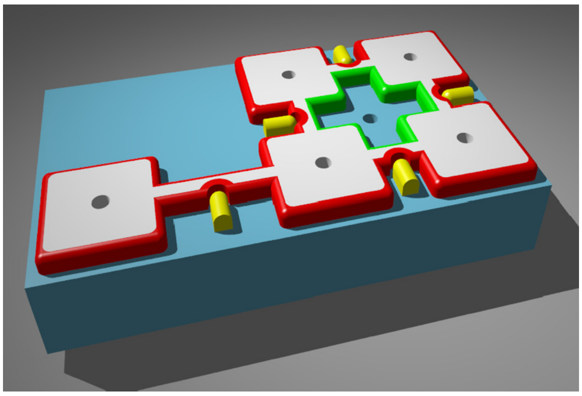

FIG. 1. (Color online) Schematic device setup of a NOT gate for the MF qubit. Finite square samples (called bricks) of the heterostructure of the ferromagnetic insulator and spin-orbit coupling semiconductor are positioned on the surface of an s-wave superconductor with vortices (black dots) trapped in it. The four bricks (on the right side) form the NOT gate. The edge MF of another brick (on the left side) can be driven to circle the vortex at the center of the loop formed by the four bricks by tuning gate voltages at the pointlike constriction junctions.

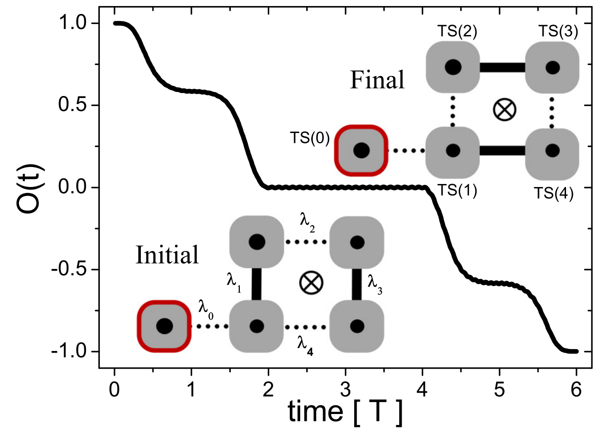

FIG. 2. (Color online) Time evolution of the MF wave function transported through the NOT gate in terms of projections $O(t)$ to its initial wave function. The time for one switching step is $T = 4\times10^4\hbar/t_0$. The two insets schematically show the initial and final stages, where the solid (dotted) lines denote the on, $\lambda = 1$ (off, $\lambda = 0$) state of the constriction junctions between TSs.

safely) and thus will be omitted hereafter. The linear dimension of TSs should be chosen appropriately [33]: for too large TSs, the energy gap between the zero-energy MF state and the lowest excited state becomes very small, which limits the operation temperature, while for too small TSs the core MF and edge MF interact with each other, which destroys the zero-energy MF ground state. Edge MFs interact with neighboring ones through the constriction junctions when electron hoppings are permitted. There is an additional vortex in the s-SC substrate inside the loop formed by the four TSs, which governs the interactions among edge MFs as will be revealed below. We attach a MF qubit to the above device as schematically shown in Fig. 1.

The low-energy physics of the system can be described by the following effective Hamiltonian:

$$\hat{H}_{\rm MF} = i\lambda_0(t)\Gamma_0\hat{\gamma}_0\hat{\gamma}_1 + i\sum_{j=1,4}\lambda_j(t)\Gamma_j\hat{\gamma}_j\hat{\gamma}_{j+1}, \quad (1)$$

where $\hat{\gamma}_0$ denotes the edge MF at the qubit, and $\hat{\gamma}_j$ with $1 \leqslant j \leqslant 4$ denote those on the TSs in the NOT gate and $\hat{\gamma}_5 \equiv \hat{\gamma}_1$; time-dependent dimensionless factors $0 \leqslant \lambda_j(t) \leqslant 1$ are introduced for the switching process of constriction junctions, whereas Γ_j are the MF interactions when the gate voltage is off and thus two TSs are connected fully.

At the initial stage, the switch configuration is described by the vector $(\lambda_0,\lambda_1,\lambda_2,\lambda_3,\lambda_4) = (0,1,0,1,0)$ (see the left inset of Fig. 2). There is an edge MF $\hat{\gamma}_0$ localized at the qubit since it is disconnected from other TSs [33]. In contrast, with $\lambda_1 = \lambda_3 = 1$, both the unified edge of TS(1) and TS(2) and that of TS(3) and TS(4) contain two vortices, and thus there is no edge MF in the NOT gate. This can be seen from Eq. (1) since the MFs $\hat{\gamma}_j$ for $1 \leqslant j \leqslant 4$ are fused to finite energies due to nonzero interactions.

Turning on the connection between the qubit and TS(1), namely, $\lambda_0 = 0 \to 1$, the wave function of $\hat{\gamma}_0$ spreads to the unified edge of the now connected qubit, TS(1) and TS(2), since the unified edge contains three vortices [33]. We then turn off the connection between TS(1) and TS(2), namely, $\lambda_1 = 1 \to 0$. The wave function of the edge MF collapses totally on TS(2) due to the topological property as revealed in the previous work [33]. After these two switchings, the edge MF $\hat{\gamma}_0$ is transported completely to TS(2). Repeating this process, one can drive the edge MF $\hat{\gamma}_0$ through the NOT gate in a clockwise way and return it back to the initial position at the qubit, with the switching sequence $(0,1,0,1,0) \mapsto (1,1,0,1,0) \mapsto (1,0,0,1,0) \mapsto (1,0,1,1,0) \mapsto (1,0,1,0,0) \mapsto (1,0,1,0,1) \mapsto (0,0,1,0,1)$. During this process the edge MF feels the gauge field formed by the central vortex and thus acquires a phase of π which makes $\hat{\gamma}_0 \mapsto -\hat{\gamma}_0$. As a result, the electronic parity of the qubit is flipped.

In order to confirm the function of the NOT gate, we consider the following microscopic Hamiltonian:

$$H_0 = \int d\vec{r}\hat{c}^\dagger(\vec{r})\left[\frac{\overrightarrow{p}^2}{2m^*} - \mu + \alpha_R(\overrightarrow{\sigma}\times\overrightarrow{p})\cdot\hat{z} + V_z\hat{\sigma}_z\right]\hat{c}(\vec{r}), \quad (2)$$

with m^*, μ, α_R, and V_z being the effective electron mass, chemical potential, strength of the Rashba spin-orbit coupling, and Zeeman field, respectively; $\vec{\sigma} = (\hat{\sigma}_x,\hat{\sigma}_y,\hat{\sigma}_z)$ being the Pauli matrices; and $\tilde{c} = (\hat{c}_\uparrow,\hat{c}_\downarrow)^{\rm T}$ being the electron annihilation operators. Superconductivity in the semiconductor induced by a superconducting substrate is $H_{\rm SC} = \int d\vec{r}[\Delta(\vec{r})\hat{c}_\uparrow^\dagger(\vec{r})\hat{c}_\downarrow^\dagger(\vec{r}) +$ H.c.], where $\Delta(\vec{r})$ is the effective pairing potential.

The quasiparticle excitations are described by the BdG equation:

$$\begin{pmatrix} H_0 & \Delta \\ \Delta^\dagger & -\hat{\sigma}_y H_0^* \hat{\sigma}_y \end{pmatrix}\Psi(\vec{r}) = E\Psi(\vec{r}), \quad (3)$$

where the Nambu spinor notation $\Psi(\vec{r}) = [u_\uparrow(\vec{r}),u_\downarrow(\vec{r}), v_\downarrow(\vec{r}), -v_\uparrow(\vec{r})]$ is adopted. With the particle-hole symmetry, one finds that any eigenvector Ψ of Eq. (3) with energy E has its counterpart $\hat{\sigma}_y\hat{\tau}_y\Psi^*$ with energy $-E$, where $\hat{\tau}_y$ is the Pauli matrix in Nambu spinor space. Because the BdG Hamiltonian is even dimensional, zero-energy eigenmodes should also appear in pairs. By recombining these zero-energy eigenwave functions, one can always achieve $\Psi = \hat{\sigma}_y \hat{\tau}_y \Psi^*$, for which the quasiparticle operator defined by $\hat{\gamma}^\dagger = \int d\vec{r} \sum_\sigma u_\sigma(\vec{r})\hat{c}^\dagger_\sigma(\vec{r}) + v_\sigma(\vec{r})\hat{c}_\sigma(\vec{r})$ satisfies the relation $\hat{\gamma}^\dagger = \hat{\gamma}$. Therefore, the zero-energy excitations of the system are actually pairs of MFs.

To investigate the dynamics of MFs in a finite system, we first derive the discrete version of the total Hamiltonian $H = H_0 + H_{\rm SC}$ on a square grid and diagonalize the tight-binding BdG Hamiltonian:

$$\begin{aligned}\tilde{H} = &-t_0 \sum_{i,j,\sigma} \hat{c}^\dagger_{i\sigma}\hat{c}_{j\sigma} - \mu \sum_{i,\sigma} \hat{c}^\dagger_{i\sigma}\hat{c}_{i\sigma} + \sum_i V_z(\hat{c}^\dagger_{i\uparrow}\hat{c}_{i\uparrow} - \hat{c}^\dagger_{i\downarrow}\hat{c}_{i\downarrow})\\ &+ it_\alpha \sum_{i,\delta} [\hat{c}^\dagger_{i+\delta_x}\hat{\sigma}_y\hat{c}_i - \hat{c}^\dagger_{i+\delta_y}\hat{\sigma}_x\hat{c}_i + \text{H.c.}]\\ &+ \sum_i [\Delta(\boldsymbol{i})\hat{c}^\dagger_{i\uparrow}\hat{c}^\dagger_{i\downarrow} + \text{H.c.}],\end{aligned} \tag{4}$$

where both spin-conserved hopping $t_0 = \hbar^2/2m^*a^2$ and spin-flipped hopping $t_\alpha = \alpha_R\hbar/2a$ are between nearest neighbors with a the grid spacing, and V_z is the Zeemann energy. In the present work, TSs of 300×300 nm^2 are divided into 100×100 sites and the parameters are set as $\Delta = 0.5t_0$, $t_\alpha = 0.9t_0$, and $V_z = 0.8t_0$.

As in the previous work [33], an edge MF state is obtained at the MF qubit with the wave function $|\phi_{\rm MF}\rangle \equiv |\Psi(t=0)\rangle$ at the initial state. Then we modulate dynamically the hopping parameters at the constriction junctions in Eq. (4), which simulates the switching of the gate voltages [33]. The evolution of the wave function is obtained by solving the TDBdG equation $i\hbar\frac{\partial}{\partial t}|\Psi(t)\rangle = H|\Psi(t)\rangle$, with the hopping parameters in Hamiltonian Eq. (4) varying with time at the constriction junctions, based on the Chebyshev polynomials expansion [34,35].

In order to monitor the time evolution of the edge MF, we project the time-dependent wave function onto the initial one and evaluate the parameter $O(t) = \langle\phi_{\rm MF}|\Psi(t)\rangle$. As can be seen in Fig. 2, $O(t)$ changes from positive unity at the initial stage to negative unity at the final stage, indicating a sign change in the MF wave function. It is worth noticing that the conservation of the function norm as seen in Fig. 2 confirms the topological protection of the edge MF during the operating process since adiabatic tunings of gate voltages have been carried out [33].

III. PARITY FLIPPING IN NOT GATE

Since the parity of the whole system is conserved upon application of gate voltage as well as Cooper pair tunneling from the SC substrate, the above switching operation should reverse the parities of the MF qubit and NOT gate simultaneously. In order to check the electronic parity of the NOT gate, we investigate first the signs of MF interactions Γ_j defined in Eq. (1). As revealed in a previous work [33], when $\hat{\gamma}_0$ is transported to TS(2) it picks a sign sgn$[\Gamma_0\Gamma_1]$. Therefore, the sign of the edge MF $\hat{\gamma}_0$ after being driven through the NOT gate is given in terms of the interactions by

$$\hat{\gamma}_0 \Rightarrow \text{sgn}[\Gamma_0\Gamma_1\Gamma_2\Gamma_3\Gamma_4(-\Gamma_0)]\hat{\gamma}_0, \tag{5}$$

where the minus sign attached to Γ_0 is due to the two opposite motions of MF $\hat{\gamma}_0$ during the transportation [33].

It is then clear that the sign reversal of $\hat{\gamma}_0$ implies $\Gamma_1\Gamma_2\Gamma_3\Gamma_4 > 0$, a topological property generated by the central vortex. Here we consider explicitly the case where all interactions are positive since all possible configurations of interaction signs satisfying $\prod_{j=1,4}\Gamma_j > 0$ can be transformed to each other by gauge transformation. It is worth noting that the same sign constraint $\prod_{j=1,2N}\Gamma_j > 0$ is available for an even number of TSs, which will be used for later discussions.

We define two regular electronic states with the four MFs, $\hat{d}_1^\dagger = (\hat{\gamma}_1 + i\hat{\gamma}_2)/2$ and $\hat{d}_2^\dagger = (\hat{\gamma}_3 + i\hat{\gamma}_4)/2$, as always possible even when the MFs are bounded and not free. We then rewrite Hamiltonian Eq. (1) in terms of the basis $|n_1n_2\rangle = \{|00\rangle,|11\rangle,|10\rangle,|01\rangle\}$, with n_i denoting the parity of the electronic state:

$$H_{\rm MF} = \begin{bmatrix} \Gamma_1'+\Gamma_3' & \Gamma_2'-\Gamma_4' & 0 & 0\\ \Gamma_2'-\Gamma_4' & -(\Gamma_1'+\Gamma_3') & 0 & 0\\ 0 & 0 & \Gamma_1'-\Gamma_3' & \Gamma_2'+\Gamma_4'\\ 0 & 0 & \Gamma_2'+\Gamma_4' & -(\Gamma_1'-\Gamma_3')\end{bmatrix}, \tag{6}$$

where $\Gamma_j' \equiv \lambda_j(t)\Gamma_j$. The four eigenenergies are given by $E_{1,2} = \pm\sqrt{(\Gamma_1'+\Gamma_3')^2 + (\Gamma_2'-\Gamma_4')^2}$ and $E_{3,4} = \pm\sqrt{(\Gamma_1'-\Gamma_3')^2 + (\Gamma_2'+\Gamma_4')^2}$ for even and odd parities of electron number, respectively.

The switch configuration of the constriction junctions in the NOT gate changes after the operation: $\lambda_1 = \lambda_3 = 1$ and $\lambda_2 = \lambda_4 = 0$ at the initial stage, while $\lambda_1 = \lambda_3 = 0$ and $\lambda_2 = \lambda_4 = 1$ at the final stage. It is clear that the ground-state energy $E_{\rm g} = -(\Gamma_1+\Gamma_3)$ at the initial stage is achieved in the even-parity subspace, while $E_{\rm g} = -(\Gamma_2+\Gamma_4)$ at the final stage in the odd-parity subspace. Therefore, the electronic parity of the NOT gate is reversed after the operation of switching.

In the above analysis, we take the interactions Γ_i positive. The same treatment can be carried out for other possible cases of signs, which is guaranteed by the particle-hole symmetry in the present system. It is easy to see that the parity reversal always takes place due to the relation $\Gamma_1\Gamma_2\Gamma_3\Gamma_4 > 0$, a topological property ensured by the central vortex.

IV. SINGLE ELECTRON PUMPING

The topological property of the NOT gate revealed above can be used for single electron pumping when two NOT gates are connected via one QD, as schematically displayed in Fig. 3(a). The QD is prepared in such a way that there is only one energy level on the QD, and the state of the QD is either vacant or occupied by one electron. The couplings between QD and NOT gates are tuned by gate voltages and are controlled to be small, since apparently it should not yield any disturbance to the TS beyond the minimal energy gap of quasiparticle excitations [33]. In such a case, the Coulomb blockade effect is

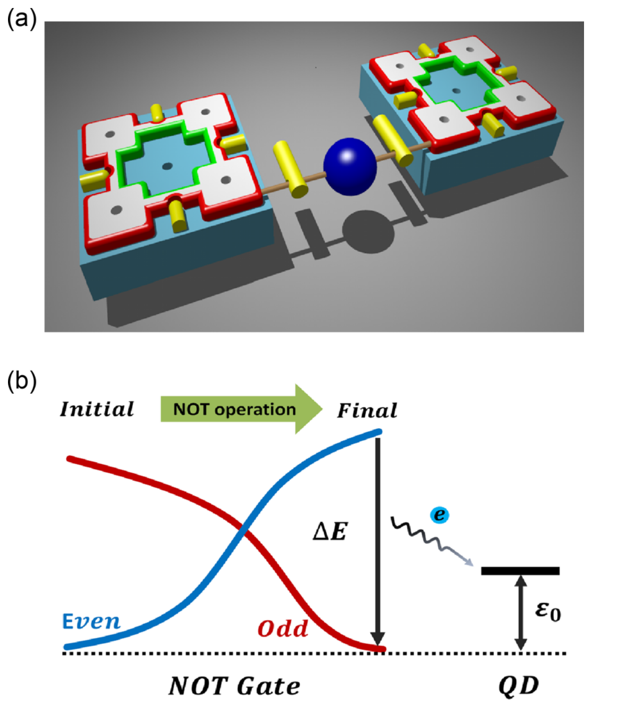

FIG. 3. (Color online) (a) Topological single electron pumping realized by two NOT gates and one QD. A gate voltage (yellow cylinder) is used to tune the coupling between the QD and one TS in the NOT gate. (b) Working mechanism of single electron pumping (see text). The two lowest energy levels (red and blue) associated with opposite parities of the NOT gate cross each other upon the switching operation, with ΔE the energy difference at the final stage. When $\Delta E > \epsilon_0$ (see text), the occupation energy of the QD, an electron is emitted from the NOT gate to the QD to lower the energy of the whole system.

limited in the QD. In the present electron pumping device, the SC substrates of NOT gates serve as the electrodes carrying the current upon electron pumping. Therefore, the charging effect in TSs can be neglected safely. Switchings are adiabatic and temperature is set low enough [33].

Let us begin with the configuration where the QD is detached from both NOT gates. Without losing generality, we consider the case of a vacant state of a QD at the initial stage, and couplings Γ_1 and Γ_3 are on whereas Γ_2 and Γ_4 are off. The subsystem of the QD and right-hand-side (rhs) NOT gate takes an even parity as discussed in the previous sections. Now we connect the QD to the rhs NOT gate and perform the same switching process formulated above for the MF qubit. The Hamiltonian is given similarly to Eq. (1) except that the first term is replaced by

$$\hat{H}_{\mathrm{QD}} = \epsilon_0 \hat{d}^\dagger \hat{d} + \Gamma_{\mathrm{QD}}(\hat{d}^\dagger \hat{\gamma}_1 + \text{c.c.}). \tag{7}$$

After the whole switching process formulated in the above section, QD is detached from the rhs NOT gate and the couplings Γ_1 and Γ_3 are off and Γ_2 and Γ_4 are on at the final stage. Due to the parity conservation concerning the subsystem of the QD and rhs NOT gate, there are two candidates for the ground state of this subsystem at the final stage: the vacant QD with total energy $-|\Gamma_2 - \Gamma_4|$ and occupied QD with total energy $-(\Gamma_2 + \Gamma_4) + \epsilon_0$, which can be obtained straightforwardly in a similar way as for Eq. (6) since at both initial and final stages Γ_{QD} is off. When $-(\Gamma_2 + \Gamma_4) + \epsilon_0 < -|\Gamma_2 - \Gamma_4|$, namely, $\epsilon_0 < 2\min\{\Gamma_2,\Gamma_4\}$, one electron on the TS is transferred to the QD. Physically the inequality means that if the occupation energy of the QD is too large, the electron could not jump to the QD, which leaves the parity of the TS remaining the same even though the switching configuration is reversed. Intriguingly, the electron can jump onto the QD whether the chemical potential of the QD is positive or negative measured from the superconducting electrode, which is presumed as zero [see Eq. (1)].

Next we connect the QD now carrying one electron to the left-hand-side (lhs) NOT gate and perform the same switching procedure. For simplicity, we presume that the two NOT gates share the same couplings. In the same way, we figure out that after the switching process with the QD detached from the lhs NOT gate the electron is transferred to the lhs NOT gate from the QD if $-(\Gamma_2 + \Gamma_4) < -|\Gamma_2 - \Gamma_4| + \epsilon_0$, namely, $\epsilon_0 > -2\min\{\Gamma_2,\Gamma_4\}$. The physical meaning of this inequality is also clear.

Now the switching configuration is that couplings Γ_1 and Γ_3 are off and Γ_2 and Γ_4 are on on both NOT gates, and the QD is disconnected. In order to continue the pumping of the single electron from the rhs NOT gate to the lhs NOT gate, namely, to generate a current in the same current direction as discussed above, we connect the QD to the rhs NOT gate and repeat the switching process. At this switch configuration, one transports the electron in a clockwise way in the loop of TSs. It is easy to see that this change of direction does not change the physics discussed above. The same discussion applies for the lhs NOT gate. One thus arrives at a condition for electron transportation $-2\min\{\Gamma_1,\Gamma_3\} < \epsilon_0 < 2\min\{\Gamma_1,\Gamma_3\}$. Therefore, the full condition for sequential one-direction single electron pumping is

$$|\epsilon_0| < 2\min\{\Gamma_1,\Gamma_2,\Gamma_3,\Gamma_4\}. \tag{8}$$

Or, more generally, the necessary and sufficient condition for a sequential single electron pumping is that half of the absolute value of the QD on-site energy is less than the minimal value of MF interactions in the two NOT gates.

The present single electron pumping is based on the unique property of the TS, in which there are two degenerate ground states associated with even and odd numbers of electrons. Implementation of the pumping is formulated with the MFs, with interactions tunable by the gate voltages. The parity flipping of the TS specifies an odd number of electrons transferring between the NOT gate and QD upon the switching operation described above, whereas the QD with a single state due to a large Coulomb blockade effect limits the charge transfer to a single electron.

It is easy to see that the present pumping process does not require equal chemical potential for the two superconducting electrodes and that the on-site energy of the QD lies between the energies of the electrodes. Interestingly, electrons can be transferred against the difference of the chemical potentials of the two electrodes, where condition Eq. (8) is understood as for the QD on-site energy measured from each of the two electrodes. The coupling constant between the QD and the TS does not appear in an explicit way in the pumping result. It

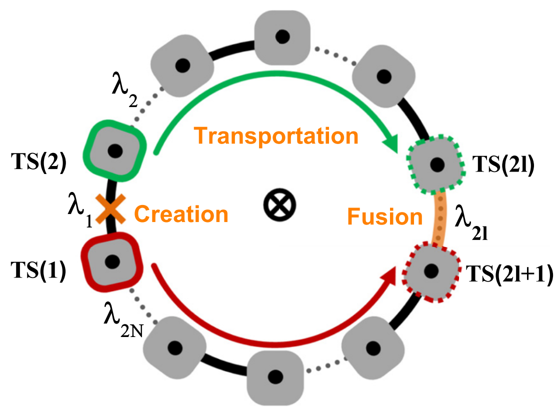

FIG. 4. (Color online) Interference of two MFs in a loop of $2N$ TSs with a central vortex. The first two MFs are created at TS(1) and TS(2) by turning off λ_1, which is denoted by the cross. These two MFs are then transported to TS($2l$) and TS($2l+1$) by turning on and off the constriction junctions on the paths. Finally, they are fused by turning on λ_{2l}.

is obvious that it should be small in order to keep the gap between the first excited state and MF states open during the whole process.

V. QUANTUM INTERFERENCE OF MFS

The parity flipping in the NOT gate discussed above can be understood generally as a quantum interference of MFs. We consider a loop of $2N$ TSs with a vortex at the center of the common superconducting substrate (see Fig. 4). The system is described by a Hamiltonian similar to Eq. (1) except the absence of the first term for the MF qubit. At the initial state, the interactions at odd and even constriction junctions are on and off, respectively, with no edge MF in the system. First, we turn off λ_1, which produces two edge MFs $\hat{\gamma}_1$ and $\hat{\gamma}_2$ on TS(1) and TS(2), respectively [33]. By turning on λ_2 and λ_{2N}, and then turning off λ_3 and λ_{2N-1}, and so on, the MF $\hat{\gamma}_2$ and $\hat{\gamma}_1$ are transported to TS($2l$) and TS($2l+1$), respectively. Finally, we turn on λ_{2l}, which annihilates the two MFs. After the above sequence of switchings, the interactions at odd and even constriction junctions become off and on, respectively, opposite to the initial configuration.

Let us check the ground-state electronic parity for the initial configuration. Since $i\Gamma_{2j-1}\hat{\gamma}_{2j-1}\hat{\gamma}_{2j} = -2\Gamma_{2j-1}\hat{d}_j^\dagger\hat{d}_j$ with $\hat{d}_j^\dagger = (\hat{\gamma}_{2j-1} + i\hat{\gamma}_{2j})/2$ for $1 \leqslant j \leqslant N$, the electronic parity operator $(-1)^{\hat{d}_j^\dagger\hat{d}_j}$ acquires the eigenvalue $-\mathrm{sgn}(\Gamma_{2j-1})$ at the ground state. The eigenvalue for electronic parity of the whole system $\hat{P} = (-1)^{\sum_{j=1,N}\hat{d}_j^\dagger\hat{d}_j} = \prod_{j=1,N}(-i\hat{\gamma}_{2j}\hat{\gamma}_{2j-1})$ reads simply $\prod_{j=1,N}[-\mathrm{sgn}(\Gamma_{2j-1})]$, since the connections between TSs are off alternatingly.

Now we evaluate the eigenvalue of parity operator $\hat{P}$ for the ground state $|\tilde{G}\rangle$ of the final configuration. With the anticommutation relations of MF operators, one can rewrite the parity operator as $\hat{P} = -\prod_{j=1,N}(-i\hat{\gamma}_{2j+1}\hat{\gamma}_{2j})$ with $\hat{\gamma}_{2N+1} = \hat{\gamma}_1$, where the additional minus sign comes from the reordering of MF operators. Following the same discussion given above for the initial configuration, the eigenvalue associated with the ground state $|\tilde{G}\rangle$ should be $-\prod_{j=1,N}[-\mathrm{sgn}(\Gamma_{2j})]$. It is then clear that the electronic parity at the ground state is reversed between the initial and final configurations due to the sign constraint of interactions $\prod_{j=1,2N}\Gamma_j > 0$. It is noticed that when the system of $2N$ TSs is isolated the parity should be preserved, and thus the true ground state with reversed parity cannot be achieved. The attachment of a MF qubit or a QD assists the parity flipping as discussed above.

It is easy to prove that without the central vortex, or generally with an even number of vortices, a system of $2N$ TSs takes the same ground-state parity after switching since now we have a different sign constraint $\prod_{j=1,2N}\Gamma_j < 0$. Therefore, with an odd number of central vortices, the quantum interference of two MFs is *constructive*, which flips the ground-state parity, whereas with an even number of central vortices the quantum interference is *destructive*, leaving no parity change in the system.

Quantum inference of MFs was discussed for a system with a superconductor and two ferromagnets on the surface of a topological insulator [24]. The two phenomena share the same topological origin induced by the central vortex. However, in the present case the parity is reversed upon the switching process, whereas in the case addressed previously an injected electron at one lead induces either emission or absorbtion of an electron (strictly speaking, an odd number of electrons), which preserves the parity.

VI. DISCUSSIONS

In the present scheme for single electron pumping, the manipulation of edge MFs should be protected by the mini gap associated with the edge MFs, which sets the limitation of the working temperature. For TSs of typical dimension 300×300 nm^2 with 100×100 grids, $a = 3$ nm and $t_0 \sim 2$ meV $\simeq 2\Delta_0$ presuming $\Delta_0 = 1$ meV and $m^* = 2m_e$. In this case, the mini gap is estimated as $\sim$100 mK, which is accessible experimentally in these days. Since we have confirmed that the system remains stable when the switching processes are carried out within $T = 40\,000\hbar/t_0$, we conclude that 12 ns is enough to ensure the adiabatical pumping in our device. The Zeeman splitting V_z required for achieving the topological phase is 1.6 meV in our model estimated from the energy gap $\Delta_0 = 1$ meV, which can be realized by using a thin film of strong ferromagnetic insulator according to a recent work [36]. As the Rashba spin-orbital coupling is tunable by an external electrical field, it is not expected to be difficult to achieve $t_\alpha \simeq 1.8$ meV used in our estimate.

The present single electron pumping shares the "turnstile" mechanism based on the QD with previous works [9,10]. There is, however, a difference between them: in previous cases electrons are driven along the direction of bias voltage; in the present system, electrons can be pumped either along or against the difference in chemical potentials of the two electrodes, which originates from the parity property of the topological superconductor featured by the MFs. The present pumping mechanism is also different from Thouless pumpings proposed so far. To move a single electron from one electrode to the other, the present system stays in a state different from the original state as seen transparently from the switching configurations, whereas a Thouless pumping for quantized charge transfer requests a close loop in the relevant parameter space.

VII. SUMMARY

In conclusion, we reveal that the mobility of a Majorana fermion at the edge of a nanotopological superconductor induced by a vortex can be used to implement a quantum NOT gate for a Majorana qubit. The working mechanism for the NOT gate can be understood as the Aharonov-Bohm interference of two Majorana fermions. Based on this phenomenon, we formulate a scheme for topological single electron pumping. Useful applications of these devices in quantum transport and quantum computation are expected.

ACKNOWLEDGMENTS

This work was supported by the WPI Initiative on Materials Nanoarchitectonics, Ministry of Education, Culture, Sports, Science and Technology of Japan, and partially by a Grant-in-Aid for Scientific Research under the Innovative Area "Topological Quantum Phenomena" (No.25103723), Ministry of Education, Culture, Sports, Science and Technology of Japan. Q.F.L. is also supported by the NSFC under Grant No.10904092.

[1] K. von Klitzing, G. Dorda, and M. Pepper, Phys. Rev. Lett. **45**, 494 (1980); K. von Klitzing, Rev. Mod. Phys. **58**, 519 (1986).
[2] B. D. Josephson, Phys. Lett. **1**, 251 (1962); Rev. Mod. Phys. **36**, 216 (1964).
[3] S. Giblin, M. Kataoka, J. Fletcher, P. See, T. J. B. M. Janssen, J. P. Griffiths, G. A. C. Jones, I. Farrer, and D. A. Ritchie, Nat. Commun. **3**, 930 (2012), and references therein.
[4] W. Lu, Z. Ji, L. Pfeiffer, K. W. West, and A. J. Rimberg, Nature (London) **423**, 422 (2003).
[5] T. Fujisawa, T. Hayashi, Y. Hirayama, H. D. Cheong, and Y. H. Jeong, Appl. Phys. Lett. **84**, 2343 (2004).
[6] M. H. Devoret, D. Esteve, and C. Urbina, Nature (London) **360**, 547 (1992).
[7] P. W. Brouwer, Phys. Rev. B **58**, R10135 (1998).
[8] M. Switkes, C. M. Marcus, K. Campman, and A. C. Gossard, Science **283**, 1905 (1999).
[9] L. P. Kouwenhoven, A. T. Johnson, N. C. van der Vaart, C. J. P. M. Harmans, and C. T. Foxon, Phys. Rev. Lett. **67**, 1626 (1991).
[10] H. Pothier, P. Lafarge, C. Urbina, D. Esteve, and M. H. Devoret, Europhys. Lett. **17**, 249 (1992).
[11] D. J. Thouless, Phys. Rev. B **27**, 6083 (1983).
[12] S. H. Simon, Phys. Rev. B **61**, R16327 (2000).
[13] G. Moore and N. Read, Nucl. Phys. B **360**, 362 (1991).
[14] N. Read and D. Green, Phys. Rev. B **61**, 10267 (2000).
[15] D. A. Ivanov, Phys. Rev. Lett. **86**, 268 (2001).
[16] A. Y. Kitaev, Phys.-Usp. **44**, 131 (2001).
[17] A. Y. Kitaev, Ann. Phys. **303**, 2 (2003).
[18] S. Das Sarma, M. Freedman, and C. Nayak, Phys. Rev. Lett. **94**, 166802 (2005).
[19] S. Tewari, S. Das Sarma, C. Nayak, C.-W. Zhang, and P. Zoller, Phys. Rev. Lett. **98**, 010506 (2007).
[20] M. Sato, Y. Takahashi, and S. Fujimoto, Phys. Rev. Lett. **103**, 020401 (2009).
[21] S. Tewari, S. Das Sarma, and D.-H. Lee, Phys. Rev. Lett. **99**, 037001 (2007).
[22] L. Fu and C. L. Kane, Phys. Rev. Lett. **100**, 096407 (2008).
[23] F. Wilczek, Nat. Phys. **5**, 614 (2009).
[24] A. R. Akhmerov, J. Nilsson, and C. W. J. Beenakker, Phys. Rev. Lett. **102**, 216404 (2009).
[25] J. D. Sau, R. M. Lutchyn, S. Tewari and S. Das Sarma, Phys. Rev. Lett. **104**, 040502 (2010).
[26] R. M. Lutchyn, J. D. Sau, and S. Das Sarma, Phys. Rev. Lett. **105**, 077001 (2010).
[27] Y. Oreg, G. Refael, and F. von Oppen, Phys. Rev. Lett. **105**, 177002 (2010).
[28] J. Alicea, Y. Oreg, G. Refael, F. von Oppen, and M. P. A. Fisher, Nat. Phys. **7**, 412 (2011).
[29] C. Nayak, S. H. Simon, A. Stern, M. Freedman, and S. Das Sarma, Rev. Mod. Phys. **80**, 1083 (2008).
[30] J. D. Sau, D. J. Clarke, and S. Tewari, Phys. Rev. B **84**, 094505 (2011).
[31] D. J. Clarke, J. D. Sau, and S. Tewari, Phys. Rev. B **84**, 035120 (2011).
[32] M. Gibertini, R. Fazio, M. Polini, and F. Taddei, Phys. Rev. B **88**, 140508(R) (2013).
[33] Q.-F. Liang, Z. Wang, and X. Hu, Europhys. Lett. **99**, 50004 (2012).
[34] S. Roche, Phys. Rev. B **59**, 2284 (1999).
[35] Y. L. Loh, S. N. Taraskin, and S. R. Elliott, Phys. Rev. Lett. **84**, 2290 (2000).
[36] J. D. Sau, S. Tewari, R. M. Lutchyn, T. D. Stanescu, and S. Das Sarma, Phys. Rev. B **82**, 214509 (2010).